

# Niobium Oxide Nanoscrolls as Building Blocks for Dye-Sensitized Hydrogen Production from Water under Visible Light Irradiation

Kazuhiko Maeda,<sup>†</sup> Miharuru Eguchi, W. Justin Youngblood, and Thomas E. Mallouk\*

Department of Chemistry, The Pennsylvania State University, University Park, Pennsylvania 16802

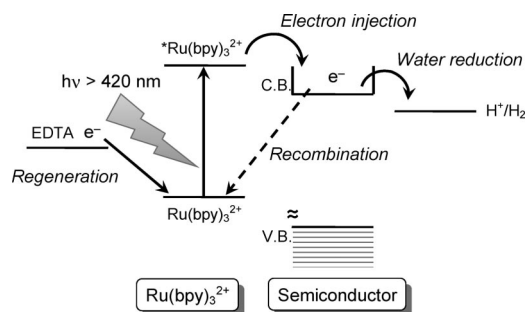
Received July 2, 2008. Revised Manuscript Received September 2, 2008

Potassium hexaniobate nanoscrolls (NS-K<sub>4</sub>Nb<sub>6</sub>O<sub>17</sub>) formed by exfoliation of lamellar K<sub>4</sub>Nb<sub>6</sub>O<sub>17</sub> were studied as building blocks for visible-light-driven H<sub>2</sub> production ( $\lambda > 420$  nm) from water using tris(2,2'-bipyridyl)ruthenium(II) chloride (Ru(bpy)<sub>3</sub><sup>2+</sup>) as a sensitizer and ethylenediaminetetraacetic acid (EDTA) as an electron donor. The surface of NS-K<sub>4</sub>Nb<sub>6</sub>O<sub>17</sub> is negatively charged at pH 3–11, enabling cationic Ru(bpy)<sub>3</sub><sup>2+</sup> molecules to be efficiently adsorbed onto the surface, allowing for rapid excited-state electron and subsequent H<sub>2</sub> evolution without any chemical bond linkage between the sensitizer and the oxide surface. The rate of visible light H<sub>2</sub> production in the nanoscroll-based system is 10 times higher than that of similarly sensitized K<sub>4</sub>Nb<sub>6</sub>O<sub>17</sub>. The difference can be primarily attributed to the strong adsorption of Ru(bpy)<sub>3</sub><sup>2+</sup> in the case of the nanoscrolls. The maximum photocatalytic reactivity is found over a narrow range of pH and Pt-loading. This study highlights the utility of single-crystalline oxide nanosheets as components of photosystems for visible-light-driven H<sub>2</sub> production from water.

## Introduction

In heterogeneous photocatalysis, H<sub>2</sub> production via water splitting with visible light is recognized as one of the most important reactions because of its potential for the production of clean and renewable H<sub>2</sub> fuel.<sup>1</sup> Production of H<sub>2</sub> from water by sensitization of a wide-gap semiconductor (e.g., metal-oxide) particle with visible-light-responsive dye molecules has been extensively studied for decades,<sup>2–7</sup> since the general principle of spectral photosensitization was introduced by Gerischer in 1972.<sup>8</sup> Scheme 1 illustrates the basic principle of dye-sensitized H<sub>2</sub> production from water. When sensitizer molecules absorb photon energy, they inject electrons into the conduction band of a metal oxide. The electrons are consumed by reduction of water at a catalytic particle such as Pt to form H<sub>2</sub>, while the oxidized sensitizer molecules are regenerated by accepting electrons from a donor molecule. In nonsacrificial systems, the ultimate electron donor

## Scheme 1. Schematic Illustration of Dye-Sensitized Hydrogen Production from Water



is water, but more commonly a sacrificial reagent such as EDTA is used to allow one to study the system without the complications of H<sub>2</sub>–O<sub>2</sub> recombination and catalysis of the oxygen-evolving reaction. The primary requirement for efficient H<sub>2</sub> production by dye sensitization is strong adsorption of sensitizer molecules onto the surface of a metal oxide, because the dye excited state is typically too short-lived to allow for diffusion of the molecule to the surface.<sup>4,7</sup> Ruthenium(II) tris(bipyridyl) (Ru(bpy)<sub>3</sub><sup>2+</sup>) and its derivatives have attracted considerable attention as visible light sensitizers for photocatalytic H<sub>2</sub> production.<sup>4,5,7,9,10</sup> The chemical structure of Ru(bpy)<sub>3</sub><sup>2+</sup> is shown in Figure 1A. Ru(II) polypyridyl sensitizers are anchored to the surface of a metal oxide through the bipyridyl ligands, which are functionalized

\* To whom corresponding author should be addressed. Tel: +1-814-863-9637. Fax: +1-814-863-8403. E-mail: tom@chem.psu.edu.

<sup>†</sup> Research fellow of the Japan Society of Promotion Science (JSPS).

- (1) (a) Kudo, A.; Kato, H.; Tsuji, I. *Chem. Lett.* **2004**, *33*, 1534. (b) Hoertz, P. G.; Mallouk, T. E. *Inorg. Chem.* **2005**, *44*, 6828. (c) Lee, J. S. *Catal. Surv. Asia* **2005**, *9*, 217. (d) Abe, R.; Sayama, K.; Sugihara, H. *J. Phys. Chem. B* **2005**, *109*, 16052. (e) Maeda, K.; Domen, K. *J. Phys. Chem. C* **2007**, *111*, 7851. (f) Zong, X.; Yan, H.; Wu, G.; Ma, G.; Wen, F.; Wang, L.; Li, C. *J. Am. Chem. Soc.* **2008**, *130*, 7176.
- (2) Houlding, V. H.; Grätzel, M. *J. Am. Chem. Soc.* **1983**, *105*, 5695.
- (3) Shimizu, T.; Iyoda, T.; Koide, Y. *J. Am. Chem. Soc.* **1985**, *107*, 35.
- (4) Furlong, D. N.; Wells, D.; Sasse, W. H. *J. Phys. Chem.* **1986**, *90*, 1107.
- (5) (a) Kim, Y. I.; Salim, S.; Huq, M. J.; Mallouk, T. E. *J. Am. Chem. Soc.* **1991**, *113*, 9561. (b) Kim, Y. I.; Atherton, S. J.; Brigham, E. S.; Mallouk, T. E. *J. Phys. Chem.* **1993**, *97*, 11802. (c) Saupé, G. B.; Mallouk, T. E.; Kim, W.; Schmehl, R. H. *J. Phys. Chem. B* **1997**, *101*, 2508.
- (6) Abe, R.; Sayama, K.; Arakawa, H. *J. Photochem. Photobiol., A* **2004**, *166*, 115.
- (7) (a) Bae, E.; Choi, W. *J. Phys. Chem. B* **2006**, *110*, 14792. (b) Park, H.; Choi, W. *Langmuir* **2006**, *22*, 2906.
- (8) Gerischer, H. *Photochem. Photobiol.* **1972**, *16*, 243.

- (9) (a) Balzani, V.; Moggli, L.; Manfrin, M. F.; Bolletta, F.; Gleria, M. *Science* **1975**, *189*, 852. (b) Kirch, M.; Lehn, J. -M.; Sauvage, J. P. *Helv. Chim. Acta* **1979**, *62*, 1345. (c) Keller, P.; Moradpour, A.; Amouyal, E.; Zidler, B. *J. Mol. Catal.* **1981**, *12*, 261. (d) Ghosh, P. K.; Brunschwig, B. S.; Chou, M.; Creutz, C.; Sutin, N. *J. Am. Chem. Soc.* **1984**, *106*, 4772. (e) Krishnan, C. V.; Brunschwig, B. S.; Creutz, C.; Sutin, N. *J. Am. Chem. Soc.* **1985**, *107*, 2005. (f) Ozawa, H.; Haga, M.; Sakai, K. *J. Am. Chem. Soc.* **2006**, *128*, 4926.
- (10) (a) Grätzel, M. *Acc. Chem. Res.* **1981**, *14*, 376. (b) Stipkala, J. M.; Castellano, F. N.; Heimer, T. A.; Kelly, C. A.; Livi, K. J. T.; Meyer, G. J. *Chem. Mater.* **1997**, *9*, 2341.

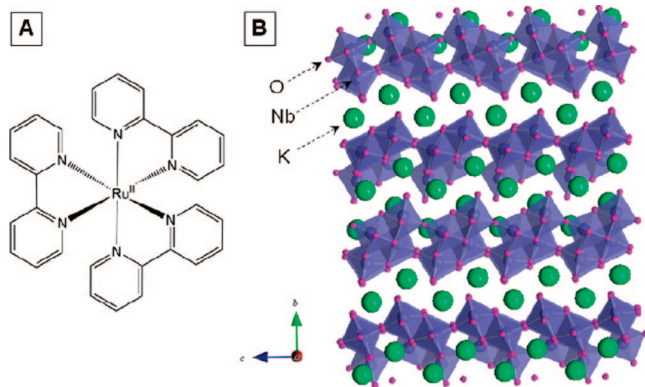


**Figure 1.** (A) Structures of Ru(bpy)<sub>3</sub><sup>2+</sup> and (B) K<sub>4</sub>Nb<sub>6</sub>O<sub>17</sub>.

typically with carboxylic acid or phosphonic acid groups. Such chemical anchoring, however, is not completely stable in aqueous solution, and the preparation of such functionalized sensitizers necessitates multistep synthetic procedures. Although surface modification of a metal-oxide semiconductor has been proposed to be a possible approach to tackle this problem,<sup>7b</sup> there still remains a challenge in dye-sensitized H<sub>2</sub> production.

Lamellar titanates and niobates consist of corner- and/or edge-shared MO<sub>6</sub> (M = Ti or Nb) octahedral units, which form a two-dimensional layered structure.<sup>11–13</sup> Each layer-sheet is negatively charged, and alkali metal cations are located between the sheets to compensate the negative charge of the layers. Certain lamellar solids undergo exfoliation upon reaction with organic bases, producing nanoscale colloidal sheets (so-called nanosheets).<sup>12–20</sup> These nanosheets are wide-gap semiconductors<sup>21</sup> and hence have been applied in heterogeneous photocatalysis including H<sub>2</sub> production from water<sup>14,22–25</sup> and photodegradation of organic compounds.<sup>26,27</sup>

Semiconductor nanosheets are attractive building blocks for preparing a photocatalytic material because of their high surface area and the wide variety of compositions available.<sup>22–27</sup>

Because the nanosheets are anionic, they are amenable to layer-by-layer restacking to produce multicomponent photosystems that incorporate electron donors, acceptors, and photon antenna molecules<sup>15</sup> and to topochemical reactions that can transform them into three-dimensionally bonded oxides<sup>17b</sup> or oxynitrides.<sup>17c</sup> Another important property of nanosheets that has not, to our knowledge, been exploited in photocatalysis is the fact that the individual lamellae are typically single crystals. This suggests that the mobility of photoinjected carriers could be relatively high, a factor that should enhance product formation relative to charge recombination in photocatalysis. Our preliminary studies of ultraviolet photocatalysis with unilamellar niobate nanoscrolls show high rates of H<sub>2</sub> production from methanol solution, consistent with this hypothesis.<sup>25b</sup> To the best of our knowledge, no attempt to apply nanosheet materials to dye-sensitized H<sub>2</sub> production has been made so far. Furthermore, the utilization of nanosheet-based materials as building blocks for visible light photoproduction of H<sub>2</sub> from water has never been attempted, although the decomposition of phenol using a hybrid photocatalyst consisting of nanoparticulate chromia and a lamellar titanate, which was prepared by exfoliation and restacking, has been reported very recently.<sup>27</sup>

In this study, we report single-sheet dye-sensitized photocatalysts derived from potassium hexaniobate (K<sub>4</sub>Nb<sub>6</sub>O<sub>17</sub>), a representative lamellar niobate that has attracted attention as a functional material with a range of interesting properties, including intercalation,<sup>28</sup> dielectric,<sup>11</sup> proton-conductive,<sup>29</sup> and photocatalytic<sup>5,14,25b,30,31</sup> properties. As shown in Figure

- (11) Nassau, K.; Shiever, J. W.; Bernstein, J. L. *J. Electrochem. Soc.* **1969**, *116*, 348.
- (12) Treacy, M. M. J.; Rice, S. B.; Jacobson, A. J.; Lewandowski, J. T. *Chem. Mater.* **1990**, *2*, 279.
- (13) (a) Sasaki, T.; Watanabe, M.; Hashizume, H.; Yamada, H.; Nakazawa, H. *J. Am. Chem. Soc.* **1996**, *118*, 8329. (b) Sasaki, T.; Ebina, Y.; Kitami, Y.; Watanabe, M.; Oikawa, T. *J. Phys. Chem. B* **2001**, *105*, 6116.
- (14) (a) Abe, R.; Shinohara, K.; Tanaka, A.; Hara, M.; Kondo, J. N.; Domen, K. *Chem. Mater.* **1997**, *9*, 2179. (b) Abe, R.; Hara, M.; Kondo, J. N.; Domen, K.; Shinohara, K.; Tanaka, A. *Chem. Mater.* **1998**, *10*, 1647.
- (15) (a) Keller, S. W.; Kim, H.-N.; Mallouk, T. E. *J. Am. Chem. Soc.* **1994**, *116*, 8817. (b) Keller, S. W.; Johnson, S. A.; Brigham, E. S.; Yonemoto, E. H.; Mallouk, T. E. *J. Am. Chem. Soc.* **1995**, *117*, 12879. (c) Kaschak, M.; Lean, J.; Waraksa, C.; Saupe, G.; Usami, H.; Mallouk, T. E. *J. Am. Chem. Soc.* **1999**, *121*, 3435.
- (16) (a) Saupe, G. B.; Waraksa, C. C.; Kim, H.-N.; Han, Y. J.; Kaschak, D. M.; Skinner, D. M.; Mallouk, T. E. *Chem. Mater.* **2000**, *12*, 1556. (b) Kobayashi, Y.; Hata, H.; Salama, M.; Mallouk, T. E. *Nano Lett.* **2007**, *7*, 2142.
- (17) (a) Schaak, R. E.; Mallouk, T. E. *Chem. Mater.* **2000**, *12*, 3427. (b) Schaak, R. E.; Mallouk, T. E. *Chem. Mater.* **2002**, *14*, 1455. (c) Schottenfeld, J. A.; Chen, G.; Eklund, P. C.; Mallouk, T. E. *J. Solid State Chem.* **2005**, *178*, 2313.
- (18) Han, Y.-S.; Park, I.; Choy, J.-H. *J. Mater. Chem.* **2001**, *11*, 1277.
- (19) Schaak, R. E.; Mallouk, T. E. *Chem. Commun.* **2002**, 706.
- (20) Du, G.; Chen, Q.; Yu, Y.; Zhang, S.; Zhou, W.; Peng, L.-M. *J. Mater. Chem.* **2004**, *14*, 1437.
- (21) (a) Sasaki, T.; Watanabe, M. *J. Phys. Chem. B* **1997**, *101*, 10159. (b) Sakai, N.; Ebina, Y.; Takada, K.; Sasaki, T. *J. Am. Chem. Soc.* **2004**, *126*, 5851.
- (22) (a) Choy, J.-H.; Lee, H.-C.; Jung, H.; Hwang, S.-J. *J. Mater. Chem.* **2001**, *11*, 2232. (b) Choy, J.-H.; Lee, H.-C.; Jung, H.; Kim, H.; Boo, H. *Chem. Mater.* **2002**, *14*, 2486.
- (23) (a) Ebina, Y.; Sasaki, T.; Harada, M.; Watanabe, M. *Chem. Mater.* **2002**, *14*, 4390. (b) Ebina, Y.; Sakai, N.; Sasaki, T. *J. Phys. Chem. B* **2005**, *109*, 17212.
- (24) (a) Compton, O. C.; Carroll, E. C.; Kim, J. Y.; Larsen, D. S.; Osterloh, F. E. *J. Phys. Chem. C* **2007**, *111*, 14589. (b) Compton, O. C.; Mullett, C. H.; Chiang, S.; Osterloh, F. E. *J. Phys. Chem. C* **2008**, *112*, 6202.
- (25) (a) Hata, H.; Kobayashi, Y.; Bojan, V.; Youngblood, W. J.; Mallouk, T. E. *Nano Lett.* **2008**, *8*, 794. (b) Ma, R.; Kobayashi, Y.; Youngblood, W. J.; Sasaki, T.; Mallouk, T. E. *J. Mater. Res.* in press.
- (26) Paek, S.-M.; Jung, H.; Lee, Y.-J.; Park, M.; Hwang, S.-J.; Choy, J.-H. *Chem. Mater.* **2006**, *18*, 1134.
- (27) Kim, T. W.; Hur, S. G.; Hwang, S.-J.; Park, H.; Choi, W.; Choy, J.-H. *Adv. Funct. Mater.* **2007**, *17*, 307.
- (28) (a) Lagaly, G.; Beneke, K. *J. Inorg. Nucl. Chem.* **1976**, *38*, 1513. (b) Kinomura, N.; Kumada, N.; Muto, F. *J. Chem. Soc., Dalton Trans.* **1985**, 2349. (c) Nakato, T.; Sakamoto, D.; Kuroda, K.; Kato, C. *Bull. Chem. Soc. Jpn.* **1992**, *65*, 322. (d) Yamaguchi, Y.; Yui, T.; Takagi, S.; Shimada, T.; Inoue, H. *Chem. Lett.* **2001**, *30*, 644. (e) Tong, Z.; Takagi, S.; Tachibana, H.; Takagi, K.; Inoue, H. *Chem. Lett.* **2005**, *34*, 608.
- (29) Eguchi, M.; Angelone, M. S.; Yennawar, H. P.; Mallouk, T. E. *J. Phys. Chem. C* **2008**, *112*, 11280.
- (30) (a) Domen, K.; Kudo, A.; Shinozaki, A.; Tanaka, A.; Maruya, K.; Onishi, T. *J. Chem. Soc., Chem. Commun.* **1986**, 356. (b) Domen, K.; Kudo, A.; Shibata, M.; Tanaka, A.; Maruya, K.; Onishi, T. *J. Chem. Soc., Chem. Commun.* **1986**, 1706. (c) Kudo, A.; Tanaka, A.; Domen, K.; Maruya, K.; Aika, K.; Onishi, T. *J. Catal.* **1988**, *111*, 67. (d) Kudo, A.; Sayama, K.; Tanaka, A.; Asakura, K.; Domen, K.; Maruya, K.; Onishi, T. *J. Catal.* **1989**, *120*, 337. (e) Sayama, K.; Tanaka, A.; Domen, K.; Maruya, K.; Onishi, T. *J. Phys. Chem.* **1991**, *95*, 1345. (f) Sayama, K.; Yase, K.; Arakawa, H.; Asakura, K.; Tanaka, A.; Domen, K.; Onishi, T. *J. Photochem. Photobiol. A* **1998**, *114*, 125.
- (31) (a) Yoshimura, J.; Kudo, A.; Tanaka, A.; Domen, K.; Maruya, K.; Onishi, T. *J. Catal.* **1988**, *147*, 401. (b) Yoshimura, J.; Tanaka, A.; Kondo, J. N.; Domen, K. *Bull. Chem. Soc. Jpn.* **1995**, *68*, 2439.

1B,  $K_4Nb_6O_{17}$  is composed of corner- and edge-shared  $NbO_6$  octahedral sheets interleaved with  $K^+$  cations for charge compensation. Following proton exchange and reaction with organic bases,  $K_4Nb_6O_{17}$  undergoes exfoliation to yield nanoscale unilamellar scrolls.<sup>16,20</sup> These scrolls are interesting as building blocks for dye-sensitized  $H_2$  production with cationic  $Ru(bpy)_3^{2+}$  molecules because of their negatively charged surface, high aspect ratio, large surface area, and single crystalline texture. The fact that  $Nb_6O_{17}^{4-}$  polyanion sheets can host catalytic active sites for  $H_2$  production<sup>30b,31</sup> also motivates us to apply them to the construction of a catalytic  $H_2$  production system. In addition, from the viewpoint of developing nonsacrificial overall water splitting systems that incorporate oxygen evolution catalysts such as iridium dioxide,<sup>1b,10a</sup> the development of a dye-sensitized sacrificial system is a first step and will give us useful information.

The present paper reports on  $K_4Nb_6O_{17}$  nanoscrolls as a building block for visible light ( $\lambda > 420$  nm)  $H_2$  production from water containing EDTA as a sacrificial electron donor using  $Ru(bpy)_3^{2+}$ , which is the simplest of the ruthenium(II) bipyridine sensitizers. To our knowledge this is the first reported attempt to use dye-sensitized nanosheets for photocatalytic  $H_2$  production from water. The essential requirements for maximizing the activity of such a system are also presented.

## Experimental Section

**Preparation of  $K_4Nb_6O_{17}$  Nanoscrolls.**  $K_4Nb_6O_{17}$  was prepared by heating a mixture of  $K_2CO_3$  (99.9%, J. T. Baker) and  $Nb_2O_5$  (99.99%, Aldrich) powders at 1473 K for 0.25 h in air (ramp rate:  $20\text{ K}\cdot\text{min}^{-1}$ ). An excess amount of  $K_2CO_3$  (10 mol % of K) was added in the mixture to compensate for volatilization. The as-obtained product was washed with water and ground into a powder using a mortar and pestle. Proton exchange was carried out in aqueous sulfuric acid (100 mL, 0.5 N) at room temperature for 24 h. The degree of cation exchange was determined by atomic absorption spectrometry to be about 50% ( $H/K \approx 1$ ).<sup>29</sup> The  $H^+$ -exchanged product is abbreviated as  $H^+/K_4Nb_6O_{17}$  hereafter. Nanoscrolls derived from  $Nb_6O_{17}^{4-}$  sheets were prepared by shaking the  $H^+/K_4Nb_6O_{17}$  in aqueous tetra(*n*-butyl)ammonium hydroxide ( $TBA^+OH^-$ , Alfa Aesar, 125 mL, 8 wt %) at room temperature for 24 h. The resulting suspension was centrifuged, and the precipitate was removed from the suspension, yielding a colloidal suspension of  $Nb_6O_{17}^{4-}$  nanoscrolls.<sup>16a</sup> The nanosheet colloid was precipitated by adding aqueous hydrochloric acid (HCl) or nitric acid ( $HNO_3$ ). The resulting solid was then rinsed several times with pure water to remove excess HCl or  $HNO_3$  and is hereafter referred to as NS- $K_4Nb_6O_{17}$  (NS = nanoscroll) for simplicity.

**Modification with Platinum Nanoparticles.** Nanoparticles of platinum (Pt) as a catalyst for  $H_2$  evolution were loaded by an *in situ* photodeposition method.<sup>32</sup> In a typical preparation, an aqueous solution (10 mL) containing the appropriate amount of  $H_2PtCl_6$  and methanol (1 mL, 10 vol %) was irradiated with ultraviolet (UV) light ( $\lambda > 300$  nm) under argon bubbling for 2 h. After irradiation, the resulting solids were washed with water and collected by centrifugation. Finally, the sample was dried in an oven at 333 K overnight.

In the case of loading Pt onto  $H^+/K_4Nb_6O_{17}$ , the as-prepared  $K_4Nb_6O_{17}$  powder (50 mg) was stirred magnetically in an aqueous solution (9 mL) containing a cationic Pt-precursor,  $[Pt(NH_3)_4]Cl_2$ , (99.995%, Alfa Aesar) for 3 days so as to intercalate the  $[Pt(NH_3)_4]^{2+}$  ions into the interlayer galleries of  $K_4Nb_6O_{17}$ .<sup>30e</sup> Then, methanol (1 mL) was added to the solution followed by irradiation with UV light ( $\lambda > 300$  nm) under argon bubbling for 16 h to reduce the intercalated cations to metallic Pt.<sup>30f</sup> The product was then subjected to proton-exchange with 0.5 N aqueous  $H_2SO_4$  at room temperature for 24 h in a manner similar to that described above. It has been shown that  $H^+/K_4Nb_6O_{17}$  exhibits much higher UV activity for  $H_2$  photoproduction than  $K_4Nb_6O_{17}$ , because proton exchange causes hydration of the interlayer galleries.<sup>30b</sup>

**Characterization of Materials.** Powder X-ray diffraction (XRD) patterns were obtained with a Philips X'Pert MPD diffractometer using Cu  $K\alpha$  radiation, and transmission electron micrographs (TEM) were obtained using a Jeol JEM-1200EX II microscope. Zeta-potential measurements were performed with a Brookhaven Instruments Zeta PALS at 298 K. To measure the pH dependence of the zeta-potential, the pH was adjusted by addition of aqueous HCl or sodium hydroxide (NaOH) solutions.

**Adsorption Measurements.** Adsorption of tris(2,2'-bipyridyl)-ruthenium(II) chloride ( $Ru(bpy)_3^{2+}$ ; 99.95%, Aldrich) onto the  $K_4Nb_6O_{17}$ -based materials was performed at room temperature. The appropriate powder (5.0 mg) was dispersed in an aqueous solution (2.0 mL) containing  $Ru(bpy)_3^{2+}$  under continuous stirring in the dark to establish adsorption-desorption equilibrium. The pH of the suspension was adjusted by HCl or NaOH as necessary. After 1 h, the solid was separated from 1.5 mL of the suspension by centrifugation. The resulting supernatant (0.75 mL) was diluted with  $H_2O$  to 2.5 mL and was then analyzed by using a UV-visible spectrometer (Hewlett-Packard, 8452A diode array spectrophotometer). The amount of adsorbed  $Ru(bpy)_3^{2+}$  was calculated from the difference in absorbance between the initial solution and the supernatant of the sensitizer-containing solution.

**Hydrogen Production Reaction.** The reaction was performed by dispersing 5.0 mg of the  $K_4Nb_6O_{17}$ -based material in an aqueous solution (2.0 mL) containing both 10 mM ethylenediaminetetraacetic acid disodium salt dihydrate (EDTA; 99.95%, Aldrich) as an electron donor and 50  $\mu\text{M}$   $Ru(bpy)_3^{2+}$  sensitizer using a Pyrex reaction cell (10 mL capacity) sealed with a rubber septum. The reactant solution was purged with argon for 5–10 min to remove dissolved air and was then placed in an outer glass jacket where argon gas flowed continuously, to prevent air contamination during reaction. After that, the reaction vessel was irradiated with a 300 W xenon lamp fitted with a cutoff filter ( $\lambda > 420$  nm). Under these conditions, the  $K_4Nb_6O_{17}$  component does not undergo photoexcitation because the band gap is too wide to absorb visible photons.<sup>30,31</sup> The evolved gases were analyzed by gas chromatography with a thermal conductivity detector and molecular sieve 5A columns at ambient temperature. The reproducibility of the rate of  $H_2$  evolution in this system was confirmed to be within  $\sim 15\%$  under the same reaction conditions.

The turnover number (TON) for  $H_2$  production with respect to the sensitizer was estimated as

$$\text{TON} = 2H/S \quad (1)$$

where  $H$  and  $S$  represent the number of moles of  $H_2$  produced and  $Ru(bpy)_3^{2+}$  used in the reaction, respectively. We assumed that  $H_2$  production takes place when two protons react with electrons injected from the excited  $Ru(bpy)_3^{2+}$  molecules. Since some fraction of  $Ru(bpy)_3^{2+}$  and/or the oxidized  $Ru(bpy)_3^{2+}$  (i.e.,  $Ru(bpy)_3^{3+}$ ) are photodegraded to a mixture of products that include carbon dioxide and  $Ru(bpy)_3OH^{2+}$ ,<sup>9d</sup> it should be noted that the TON calculated from eq 1 is a lower limit.



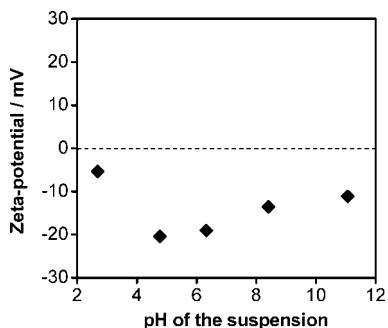


**Figure 2.** Zeta-potential of NS-K<sub>4</sub>Nb<sub>6</sub>O<sub>17</sub> as a function of the pH of the suspension. The pH was adjusted by addition of aqueous HCl or NaOH.

The apparent quantum yield (AQY) was measured using the same experimental setup but with a band-pass filter ( $\lambda = 450 \pm 20$  nm) and was estimated as

$$\text{AQY (\%)} = (2R/I) \times 100 \quad (2)$$

where  $R$  and  $I$  represent the rate at which H<sub>2</sub> molecules are evolved and the rate at which photons impinge on the sample, respectively. The AQY values are uncorrected for reflection and scattering losses and for the optical density of sensitizer molecules in the solution. The internal quantum yield per absorbed photon is thus higher than the measured value of AQY. The flux of incident photons was measured using a power meter.

## Results and Discussion

**Characterization of NS-K<sub>4</sub>Nb<sub>6</sub>O<sub>17</sub>.** The structural transformation of K<sub>4</sub>Nb<sub>4</sub>O<sub>17</sub> to nanoscrolls was confirmed by XRD patterns and TEM images, which have been discussed in previous papers<sup>16</sup> and are reported briefly in the present study as Supporting Information. XRD patterns showed that exfoliation of H<sup>+</sup>/K<sub>4</sub>Nb<sub>6</sub>O<sub>17</sub> resulted in the broadening of layer lines ( $(0k0)$  reflections), but the (040) diffraction peak remained observable at  $2\theta = 10.9$  (Figure S1, Supporting Information). This indicates that ordering along the stacking axis of K<sub>4</sub>Nb<sub>6</sub>O<sub>17</sub> is to some extent restored when the unilamellar colloid is precipitated as nanoscrolls. The peak at  $2\theta = 28$ , which is assigned to the (002) reflection, became the strongest peak, and the (220) peak was observable as well. TEM images showed the nanoscrolls with a diameter of about 30 nm and a length of a few hundred nanometers (Figure S2, Supporting Information), although there is a small fraction of unscrolled sheets in the sample.<sup>16</sup> Previous studies have confirmed that scrolling occurs preferentially along low-index directions, especially with the [100] direction as the long axis of the scroll.<sup>20</sup> The TEM data are consistent with the XRD patterns; that is, the lamellar structure of K<sub>4</sub>Nb<sub>6</sub>O<sub>17</sub> is preserved within the nanoscroll. The specific surface areas of H<sup>+</sup>/K<sub>4</sub>Nb<sub>6</sub>O<sub>17</sub> and NS-K<sub>4</sub>Nb<sub>6</sub>O<sub>17</sub> are typically 1–2 and 250–300 m<sup>2</sup>·g<sup>-1</sup>, respectively.<sup>14a,16b</sup>

Figure 2 shows the zeta-potential of the as-prepared NS-K<sub>4</sub>Nb<sub>6</sub>O<sub>17</sub> as a function of pH of the suspension. For most transition-metal metal oxides having surface hydroxyl groups (e.g., TiO<sub>2</sub>), the surface charge changes from positive to negative with increasing pH because of the ionization of M-OH groups.<sup>4,7b</sup> In contrast, the surface of NS-K<sub>4</sub>Nb<sub>6</sub>O<sub>17</sub> is negatively charged over the entire pH range examined (pH

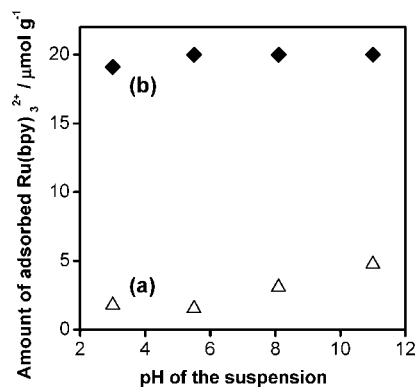


**Figure 3.** Amount of Ru(bpy)<sub>3</sub><sup>2+</sup> adsorbed on (a) H<sup>+</sup>/K<sub>4</sub>Nb<sub>6</sub>O<sub>17</sub> and (b) NS-K<sub>4</sub>Nb<sub>6</sub>O<sub>17</sub> as a function of pH of the suspension. The pH was adjusted by addition of aqueous HCl or NaOH.

3–11), indicating that NS-K<sub>4</sub>Nb<sub>6</sub>O<sub>17</sub> particles should be able to bind Ru(bpy)<sub>3</sub><sup>2+</sup> cations at all pH values relevant to water photolysis.

**Adsorption of Ru(bpy)<sub>3</sub><sup>2+</sup> Cations.** Ru(bpy)<sub>3</sub><sup>2+</sup> in aqueous solution exhibits a metal-to-ligand charge transfer (MLCT) absorption band at 400–570 nm. The intensity of the MLCT band decreased after stirring 50 μM solutions of Ru(bpy)<sub>3</sub><sup>2+</sup> with H<sup>+</sup>/K<sub>4</sub>Nb<sub>6</sub>O<sub>17</sub> or NS-K<sub>4</sub>Nb<sub>6</sub>O<sub>17</sub>, indicating that the complex is adsorbed onto these materials. The amount of adsorbed Ru(bpy)<sub>3</sub><sup>2+</sup> on H<sup>+</sup>/K<sub>4</sub>Nb<sub>6</sub>O<sub>17</sub> and NS-K<sub>4</sub>Nb<sub>6</sub>O<sub>17</sub> as a function of pH of the suspension can be estimated by UV–visible spectroscopy and is plotted in Figure 3. Although the complex adsorbs on both H<sup>+</sup>/K<sub>4</sub>Nb<sub>6</sub>O<sub>17</sub> and NS-K<sub>4</sub>Nb<sub>6</sub>O<sub>17</sub>, the adsorption behaviors were obviously different. With H<sup>+</sup>/K<sub>4</sub>Nb<sub>6</sub>O<sub>17</sub>, the amount adsorbed tended to gradually increase with increasing pH, consistent with a gradual increase of negative surface charge. In contrast, Ru(bpy)<sub>3</sub><sup>2+</sup> was almost quantitatively adsorbed on NS-K<sub>4</sub>Nb<sub>6</sub>O<sub>17</sub> over entire range of pH examined (pH 3–11). This striking difference is attributable to the fact that Ru(bpy)<sub>3</sub><sup>2+</sup> cannot easily displace protons in the interlayer galleries of H<sup>+</sup>/K<sub>4</sub>Nb<sub>6</sub>O<sub>17</sub>. It has been reported that Ru(bpy)<sub>3</sub><sup>2+</sup> molecules intercalate readily after preintercalation of the solid with alkylammonium ions<sup>28c</sup> or methylviologen.<sup>28e</sup> In the present case, however, Ru(bpy)<sub>3</sub><sup>2+</sup> molecules are adsorbed only on the external surface. XRD patterns of samples before and after adsorption showed no sign of intercalation (data not shown). Therefore, Ru(bpy)<sub>3</sub><sup>2+</sup>, a cationic sensitizer molecule, can be effectively adsorbed on NS-K<sub>4</sub>Nb<sub>6</sub>O<sub>17</sub> but not on H<sup>+</sup>/K<sub>4</sub>Nb<sub>6</sub>O<sub>17</sub>. It was also confirmed by XRD that the position of the (040) diffraction peak in NS-K<sub>4</sub>Nb<sub>6</sub>O<sub>17</sub> remains unchanged upon adsorption of Ru(bpy)<sub>3</sub><sup>2+</sup>, indicating that Ru(bpy)<sub>3</sub><sup>2+</sup> molecules are not accommodated in the stacking sheet structure of the nanoscroll but are adsorbed on the external surface. Since adsorption of sensitizer molecules is essential requirement for dye-sensitized H<sub>2</sub> production,<sup>4,7</sup> the fact that Ru(bpy)<sub>3</sub><sup>2+</sup> is effectively adsorbed onto NS-K<sub>4</sub>Nb<sub>6</sub>O<sub>17</sub> over a wide pH range (pH 3–11) is favorable for use of NS-K<sub>4</sub>Nb<sub>6</sub>O<sub>17</sub> and Ru(bpy)<sub>3</sub><sup>2+</sup> as components of a visible-light-driven system for H<sub>2</sub> production.

## Comparison of Photocatalytic Hydrogen Evolution From Dye-Sensitized NS-K<sub>4</sub>Nb<sub>6</sub>O<sub>17</sub> and H<sup>+</sup>/K<sub>4</sub>Nb<sub>6</sub>O<sub>17</sub>.

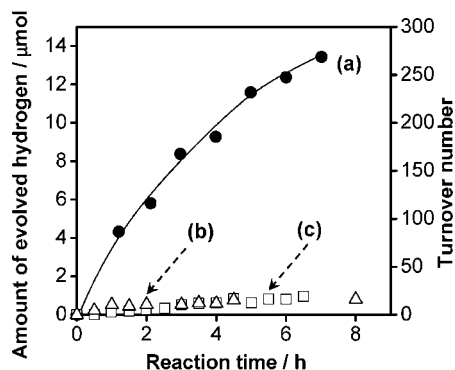


**Figure 4.** Time courses of H<sub>2</sub> evolution from 0.1 wt % Pt-loaded (a) NS-K<sub>4</sub>Nb<sub>6</sub>O<sub>17</sub> and (b) H<sup>+</sup>/K<sub>4</sub>Nb<sub>6</sub>O<sub>17</sub> sensitized by Ru(bpy)<sub>3</sub><sup>2+</sup> with visible light ( $\lambda > 420$  nm). Reaction conditions: catalyst, 5.0 mg; aqueous solution (2.0 mL) containing 10 mM EDTA and 50  $\mu$ M Ru(bpy)<sub>3</sub><sup>2+</sup>; light source, xenon lamp (300 W) with a cutoff filter. (c) Data for Pt-loaded P25 titania is also shown for comparison.

**Table 1.** H<sub>2</sub> Evolution Activities ( $\lambda > 420$  nm)<sup>a</sup> and Ru(bpy)<sub>3</sub><sup>2+</sup> Adsorption Amount

entry	material	activity, $\mu$ mol h <sup>-1</sup>	amount of adsorbed Ru(bpy) <sub>3</sub> <sup>2+</sup> , $\mu$ mol g <sup>-1</sup>
1	NS-K <sub>4</sub> Nb <sub>6</sub> O <sub>17</sub>	3.6	20
2	H <sup>+</sup> /K <sub>4</sub> Nb <sub>6</sub> O <sub>17</sub>	0.3	3.9
3	P25 titania	0.2	2.5
4 <sup>b</sup>	NS-K <sub>4</sub> Nb <sub>6</sub> O <sub>17</sub>	3.6	20
5	NS-K <sub>4</sub> Nb <sub>6</sub> O <sub>17</sub>	1.8	4.0 <sup>c</sup>

<sup>a</sup> Reaction conditions: catalyst, 5.0 mg (0.1 wt % Pt); aqueous solution containing 10 mM EDTA and 50  $\mu$ M Ru(bpy)<sub>3</sub><sup>2+</sup> (2.0 mL).  
<sup>b</sup> Ru(bpy)<sub>3</sub><sup>2+</sup> sensitizers were adsorbed on 0.1 wt % Pt-loaded NS-K<sub>4</sub>Nb<sub>6</sub>O<sub>17</sub> before mixing with aqueous EDTA solution (10 mM).  
<sup>c</sup> 10  $\mu$ M Ru(bpy)<sub>3</sub><sup>2+</sup> in the reaction solution.

Time courses of H<sub>2</sub> production using NS-K<sub>4</sub>Nb<sub>6</sub>O<sub>17</sub> and lamellar K<sub>4</sub>Nb<sub>6</sub>O<sub>17</sub> (H<sup>+</sup>/K<sub>4</sub>Nb<sub>6</sub>O<sub>17</sub>) sensitized by Ru(bpy)<sub>3</sub><sup>2+</sup> with visible light ( $\lambda > 420$  nm) are shown in Figure 4. Data for P25 titania,<sup>33</sup> which is widely recognized as one of the best materials for many photocatalytic reactions, is also shown for comparison. In all cases, Pt nanoparticles (0.1 wt %) were deposited to catalyze H<sub>2</sub> production, and the reaction pH was not controlled (initial pH 5.5). Although H<sub>2</sub> production was observed for all systems examined, the activity of the NS-K<sub>4</sub>Nb<sub>6</sub>O<sub>17</sub> system (curve (a)) was 10 times higher than those of H<sup>+</sup>/K<sub>4</sub>Nb<sub>6</sub>O<sub>17</sub> (curve (b)) and P25 (curve (c)). The difference in activity is primarily attributed to the higher affinity of NS-K<sub>4</sub>Nb<sub>6</sub>O<sub>17</sub> for Ru(bpy)<sub>3</sub><sup>2+</sup>. Table 1 compares the amounts of Ru(bpy)<sub>3</sub><sup>2+</sup> on these three materials with the H<sub>2</sub> production rates. The adsorption of Ru(bpy)<sub>3</sub><sup>2+</sup> in the case of NS-K<sub>4</sub>Nb<sub>6</sub>O<sub>17</sub> results in a higher quantum yield of charge injection from the MLCT excited state, which leads to a higher H<sub>2</sub> evolution rate. When a reaction was carried out by dispersing Pt-loaded NS-K<sub>4</sub>Nb<sub>6</sub>O<sub>17</sub> preadsorbed with 0.1  $\mu$ mol of Ru(bpy)<sub>3</sub><sup>2+</sup> in aqueous EDTA solution (10 mM), the activity (entry 4) was the same as that obtained by dispersing Pt-loaded NS-K<sub>4</sub>Nb<sub>6</sub>O<sub>17</sub> in an aqueous solution containing the same amount of EDTA and Ru(bpy)<sub>3</sub><sup>2+</sup> (entry 1). This result is consistent the observed affinity of NS-

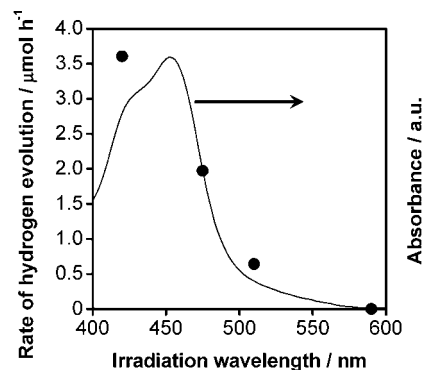


**Figure 5.** Dependence of H<sub>2</sub> evolution from 0.1 wt % Pt-loaded NS-K<sub>4</sub>Nb<sub>6</sub>O<sub>17</sub> sensitized by Ru(bpy)<sub>3</sub><sup>2+</sup> on the cutoff wavelength of the incident visible light. Reaction conditions: catalyst, 5.0 mg; aqueous solution (2.0 mL) containing 10 mM EDTA and 50  $\mu$ M Ru(bpy)<sub>3</sub><sup>2+</sup>; light source, xenon lamp (300 W) with a cutoff filter. The absorption spectrum of aqueous Ru(bpy)<sub>3</sub><sup>2+</sup> is also shown.

K<sub>4</sub>Nb<sub>6</sub>O<sub>17</sub> for Ru(bpy)<sub>3</sub><sup>2+</sup>. Similar comparisons using Pt-loaded TiO<sub>2</sub> have shown that the preadsorbed composite is more effective because EDTA displaces ruthenium-based sensitizers, thereby decreasing the sensitization efficiency.<sup>4</sup> It is important to note that NS-K<sub>4</sub>Nb<sub>6</sub>O<sub>17</sub> has substantially higher activity than H<sup>+</sup>/K<sub>4</sub>Nb<sub>6</sub>O<sub>17</sub> even when the same amount of Ru(bpy)<sub>3</sub><sup>2+</sup> (ca. 4.0  $\mu$ mol  $\cdot$  g<sup>-1</sup>) is adsorbed on both materials (entries 2 and 5). This suggests that electron transport from the excited Ru(bpy)<sub>3</sub><sup>2+</sup> molecules to the Pt nanoparticles via NS-K<sub>4</sub>Nb<sub>6</sub>O<sub>17</sub> is more facile than that via H<sup>+</sup>/K<sub>4</sub>Nb<sub>6</sub>O<sub>17</sub>. This difference may be attributed to the fact that the electron transfer pathway is in the plane of the single sheet in the case of the nanoscroll, whereas electron tunneling between sheets is likely to be important in platinized H<sup>+</sup>/K<sub>4</sub>Nb<sub>6</sub>O<sub>17</sub>. The intersheet electron transfer reaction was previously shown to be rate limiting in HI photolysis using H<sup>+</sup>/K<sub>4</sub>Nb<sub>6</sub>O<sub>17</sub>.<sup>5b,c</sup>

Figure 5 shows the dependence of the initial rate of H<sub>2</sub> production in the 0.1 wt % Pt-loaded NS-K<sub>4</sub>Nb<sub>6</sub>O<sub>17</sub>/Ru(bpy)<sub>3</sub><sup>2+</sup>/EDTA system on the wavelength of incident light, along with an absorbance spectrum of aqueous Ru(bpy)<sub>3</sub><sup>2+</sup>. The H<sub>2</sub> evolution rate decreased with increasing wavelength because of a decrease in the number of incident photons, as well as a decrease in the absorbance of Ru(bpy)<sub>3</sub><sup>2+</sup>, and finally reached zero for wavelengths longer than 590 nm. No reaction took place in the dark or when one component of the system (Pt-loaded NS-K<sub>4</sub>Nb<sub>6</sub>O<sub>17</sub>, Ru(bpy)<sub>3</sub><sup>2+</sup>, and EDTA) was absent. Thus, an electron transfer mediator, a sensitizer, and an electron donor are all indispensable for H<sub>2</sub> production in this system despite the fact that the potential of excited Ru(bpy)<sub>3</sub><sup>2+</sup> (-0.84 V vs NHE) is sufficiently negative to cause water reduction.<sup>34</sup> These results clearly indicate that the reaction is initiated by light absorption by Ru(bpy)<sub>3</sub><sup>2+</sup> and proceeds by subsequent electron transfer events according to Scheme 1. Although the lack of chemical bond linkage between Ru(bpy)<sub>3</sub><sup>2+</sup> and NS-K<sub>4</sub>Nb<sub>6</sub>O<sub>17</sub> might be disadvantageous for dye-sensitized H<sub>2</sub> production, the electrostatic attraction between the two components seems to be strong enough to promote electron injection from the excited Ru(bpy)<sub>3</sub><sup>2+</sup> molecules to the conduction band of NS-K<sub>4</sub>Nb<sub>6</sub>O<sub>17</sub> within

(33) P25 titania powder (specific surface area, ca. 55 m<sup>2</sup>  $\cdot$  g<sup>-1</sup>) was purchased from Degussa Co., and used after calcination in air at 673 K for 5 h to remove surface contamination.

(34) (a) Lin, C. T.; Böttcher, W.; Chou, M.; Creutz, C.; Sutin, N. *J. Am. Chem. Soc.* **1976**, *98*, 6536. (b) Kalyanasundaram, K. *Coord. Chem. Rev.* **1982**, *46*, 159.

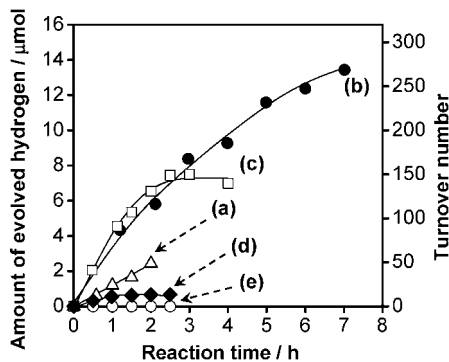
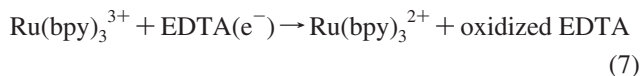
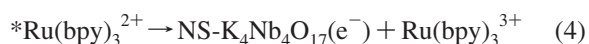
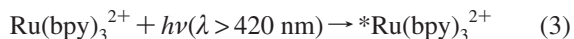


**Figure 6.** Time courses of H<sub>2</sub> evolution from 0.1 wt % Pt-loaded NS-K<sub>4</sub>Nb<sub>6</sub>O<sub>17</sub> sensitized by Ru(bpy)<sub>3</sub><sup>2+</sup> with visible light ( $\lambda > 420$  nm) at initial pH values of (a) 3.0, (b) 5.5, (c) 8.2, (d) 9.4, and (e) 11. Reaction conditions: catalyst, 5.0 mg; aqueous solution (2.0 mL) containing 10 mM EDTA and 50  $\mu$ M Ru(bpy)<sub>3</sub><sup>2+</sup>; light source, xenon lamp (300 W) with a cutoff filter.

the MLCT lifetime, which is typically several hundred nanoseconds.

**Dependence of Photocatalytic Activity on pH.** Figure 6 shows time courses of H<sub>2</sub> evolution from 0.1 wt % Pt-loaded NS-K<sub>4</sub>Nb<sub>6</sub>O<sub>17</sub> sensitized by Ru(bpy)<sub>3</sub><sup>2+</sup> with visible light ( $\lambda > 420$  nm) at various values of initial pH. The activity was found to be strongly dependent on pH. The activity increased by a factor of 3 as the pH was increased from 3.0 to 5.5. Increasing the pH above 5.5 resulted in lower activity and tended to accelerate deactivation with irradiation time, although the initial rate of H<sub>2</sub> production at pH 8.2 was the same as that obtained at pH 5.5. At pH 11, no H<sub>2</sub> evolution was observed.

As illustrated in Scheme 1, H<sub>2</sub> production in this system proceeds according to the following primary steps:



Assuming efficient charge injection from \*Ru(bpy)<sub>3</sub><sup>2+</sup> in eq 4, the quantum yield represents a kinetic competition between back reaction 4a and electron transfer reaction 7. Two molecules of Ru(bpy)<sub>3</sub><sup>2+</sup> are oxidized per molecule of H<sub>2</sub> generated, and two molecules of EDTA per H<sub>2</sub> are needed in eq 7 to maintain the catalytic cycle.<sup>7b</sup> If this reaction scheme were not regenerative, H<sub>2</sub> production should cease after 0.05  $\mu$ mol, because the amount of sensitizer added to the reactant solution was 0.1  $\mu$ mol (50  $\mu$ M, 2.0 mL). The amount of H<sub>2</sub> produced in each run except for pH 11 far exceeds this level, confirming that the system is catalytic. The TON of H<sub>2</sub> production after 7 h of reaction at pH 5.5 reached 270.

In TiO<sub>2</sub>/Ru(bpy)<sub>3</sub><sup>2+</sup>-based sensitizer/EDTA systems, it has been shown that a plot of H<sub>2</sub> production rate as a function of pH tends to follow the pH-dependent adsorption behavior

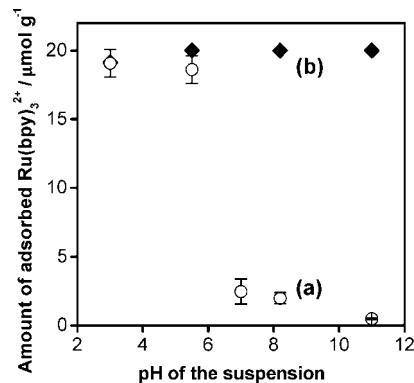


**Figure 7.** Amount of Ru(bpy)<sub>3</sub><sup>2+</sup> adsorbed on NS-K<sub>4</sub>Nb<sub>6</sub>O<sub>17</sub> as a function of pH of the suspension (a) with or (b) without 10 mM EDTA.

of the sensitizer employed.<sup>4,7</sup> In the present case, however, there is no distinct correspondence between activity and adsorption with respect to pH (Figures 3 and 6). To investigate the origin of the pH dependent H<sub>2</sub> production rate, adsorption experiments of Ru(bpy)<sub>3</sub><sup>2+</sup> on NS-K<sub>4</sub>Nb<sub>6</sub>O<sub>17</sub> were carried out in the presence of EDTA, because EDTA has been reported to hinder the adsorption of ruthenium-based sensitizer molecules on metal-oxide surfaces and even to displace sensitizer molecules adsorbed on the surface.<sup>4</sup> Figure 7 shows the amount of Ru(bpy)<sub>3</sub><sup>2+</sup> adsorbed on NS-K<sub>4</sub>Nb<sub>6</sub>O<sub>17</sub> as a function of pH in the presence of 10 mM EDTA, which is the concentration used in the reaction. Dye adsorption is only slightly suppressed at acidic pH (3–5.5) in the presence of EDTA, but the amount adsorbed was reduced significantly at neutral and basic pH (7.0–11). For metal oxides such as TiO<sub>2</sub>, EDTA is known to adsorb on the surface at low pH, in part because of electrostatic attraction to the positively charged metal oxide surface.<sup>4,7a</sup> The observed adsorption behavior of NS-K<sub>4</sub>Nb<sub>6</sub>O<sub>17</sub> with Ru(bpy)<sub>3</sub><sup>2+</sup> at pH 3.0–5.5 can be reasonably understood in terms of the zeta-potential measurements (Figure 2), which showed that the surface of NS-K<sub>4</sub>Nb<sub>6</sub>O<sub>17</sub> is negatively charged. This behavior is unusual as compared to bulk oxides and seems to be a unique and useful feature of the niobate nanoscrolls. At basic pH, EDTA exists as a trianion and should not be adsorbed on the negatively charged NS-K<sub>4</sub>Nb<sub>6</sub>O<sub>17</sub> surface because of electrostatic repulsion. It is likely that in basic solution EDTA interacts not with the NS-K<sub>4</sub>Nb<sub>6</sub>O<sub>17</sub> surface but with Ru(bpy)<sub>3</sub><sup>2+</sup>, thereby suppressing the adsorption of Ru(bpy)<sub>3</sub><sup>2+</sup> on NS-K<sub>4</sub>Nb<sub>6</sub>O<sub>17</sub>. The third acid dissociation constant of EDTA (pK<sub>a3</sub>) is 6.1–6.2,<sup>35</sup> which corresponds well to the pH at which an abrupt drop in the amount of adsorbed Ru(bpy)<sub>3</sub><sup>2+</sup> is observed (Figure 7). It thus appears that the interaction of triply ionized EDTA with Ru(bpy)<sub>3</sub><sup>2+</sup> is responsible for the decrease in photocatalytic activity above pH 5.5. The reason for deactivation of the photocatalyst with time will be discussed below.

The cause of the decrease in activity from pH 5.5 to 3.0 seems to be more complex. Since the redox potential of Ru(bpy)<sub>3</sub><sup>2+</sup> is insensitive to pH, the driving force of electron injection and H<sub>2</sub> production should increase with decreasing pH because of the positive shift of the conduction band edge potential of NS-K<sub>4</sub>Nb<sub>6</sub>O<sub>17</sub> and the water reduction potential

(35) Serjeant, E. P.; Dempsey, B. *Ionization Constants of Organic Acids in Aqueous Solution*; Pergamon Press: Oxford, 1979.



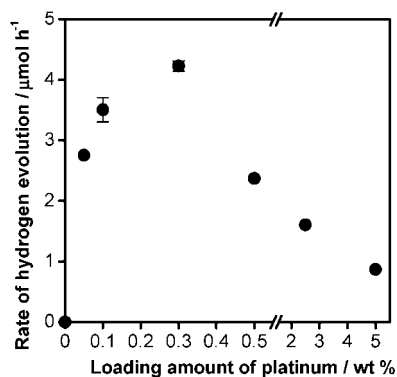


**Figure 8.** Dependence of H<sub>2</sub> evolution from 0.1 wt % Pt-loaded NS-K<sub>4</sub>Nb<sub>6</sub>O<sub>17</sub> sensitized by Ru(bpy)<sub>3</sub><sup>2+</sup> with visible light ( $\lambda > 420$  nm) on the loading Pt. Reaction conditions: catalyst, 5.0 mg; aqueous solution (2.0 mL, pH 5.5) containing 10 mM EDTA and 50  $\mu$ M Ru(bpy)<sub>3</sub><sup>2+</sup>; light source, xenon lamp (300 W) with a cutoff filter.

(Scheme 1).<sup>36</sup> On the other hand, the driving force for recombination between electrons in the conduction band of NS-K<sub>4</sub>Nb<sub>6</sub>O<sub>17</sub> and Ru(bpy)<sub>3</sub><sup>3+</sup> (reaction 4a) should decrease along with decreasing pH (Scheme 1).<sup>36</sup> These cooperative trends in the driving forces of forward/backward electron transfer reactions would lead one to predict an increase in H<sub>2</sub> production with decreasing pH. However, the photocatalytic activity was found to decrease with decreasing pH (Figure 6). The possibility that EDTA hinders the adsorption of Ru(bpy)<sub>3</sub><sup>2+</sup> at acidic pH by competitive adsorption<sup>4,7a</sup> is of course precluded by the results shown in Figure 7, which shows that adsorption of Ru(bpy)<sub>3</sub><sup>2+</sup> on NS-K<sub>4</sub>Nb<sub>6</sub>O<sub>17</sub> at pH 3.0 and 5.5 is suppressed very little by addition of 10 mM EDTA. One possible cause of a decrease in reaction rate at pH 3.0 is related to regeneration of Ru(bpy)<sub>3</sub><sup>2+</sup> by EDTA (reaction 7). If the reaction between Ru(bpy)<sub>3</sub><sup>3+</sup> and EDTA is slow, the fraction of photoinjected electrons that recombine via pathway 4a will increase. The observed pH dependence is consistent with the idea that the reaction of EDTA<sup>2-</sup> with adsorbed Ru(bpy)<sub>3</sub><sup>3+</sup> is too slow to compete with reaction 4a and that the active electron donor in the system must be EDTA<sup>3-</sup> or EDTA<sup>4-</sup>.

**Dependence of the Reaction Rate on the Loading of Pt.** It is generally known that loading of Pt significantly affects the efficiency of photocatalytic H<sub>2</sub> production.<sup>5b,23a,30e,f,37–42</sup> The H<sub>2</sub> production rate in the present system was also strongly dependent on the loading of Pt. Figure 8 shows the dependence of the initial rate of H<sub>2</sub> production on the amount of Pt. As mentioned in the Introduction, hexaniobate sheets intrinsically possess catalytically active sites for H<sub>2</sub> production.<sup>30b,31</sup> We therefore expected that sensitized NS-K<sub>4</sub>Nb<sub>6</sub>O<sub>17</sub> might be active for

H<sub>2</sub> production without adding catalytic metals. However, in the absence of Pt, the NS-K<sub>4</sub>Nb<sub>6</sub>O<sub>17</sub>/Ru(bpy)<sub>3</sub><sup>2+</sup>/EDTA system was completely inactive for visible-light-driven H<sub>2</sub> production even with irradiation times longer than 18 h. The rate of H<sub>2</sub> evolution increased with increasing Pt content to a maximum at 0.3 wt % and then decreased upon further loading. The AQY for H<sub>2</sub> evolution at the optimized loading was calculated to be approximately 10.5%.<sup>43</sup>

It has been reported by many researchers that the rate of H<sub>2</sub> evolution from aqueous solutions containing sacrificial electron donors is enhanced for a given photocatalyst by increasing the Pt loading but that excess loading results in reduced activity.<sup>23a,37–42</sup> Grätzel et al. have studied the rate of back electron transfer from the conduction band of TiO<sub>2</sub> to oxidized Eosin Y (sensitizer) using Pt-loaded and unloaded TiO<sub>2</sub>.<sup>44</sup> They reported that the Pt deposits on TiO<sub>2</sub> play a role in trapping conduction band electrons and thereby suppress back electron transfer from the conduction band to the oxidized sensitizer molecules. Therefore, an increase in activity with increasing Pt loading may be associated with successful competition with back electron transfer pathway as the density of active sites for H<sub>2</sub> production increases. In the range between 0.3 and 5.0 wt % Pt content, increasing the Pt loading had a negative effect on activity while concealing the positive effect. Although one might expect that high loadings of Pt could inhibit the adsorption of Ru(bpy)<sub>3</sub><sup>2+</sup>, quantitative adsorption was found experimentally even with the 5.0 wt % Pt sample. Therefore, this effect is not significant, at least up to 5.0 wt % Pt. It is likely that the decrease in activity with higher Pt loadings is associated with the size of Pt nanoparticles deposited on NS-K<sub>4</sub>Nb<sub>6</sub>O<sub>17</sub>. The color of the samples became much darker with increasing Pt loading, which is primarily due to the formation of larger Pt particles on the surface. Figure 9 shows TEM images of NS-K<sub>4</sub>Nb<sub>6</sub>O<sub>17</sub> loaded with (A) 0.3 and (B) 5.0 wt % Pt. The Pt deposits are clearly distinguishable because of the difference in electron density between platinum and niobium. The 0.3 wt % sample, which showed the highest activity (see Figure 8), exhibits relatively good dispersion of Pt nanoparticles with average size of 4–6 nm (Figure 9A), whereas large agglomerates of 30–50 nm are observed in the 5.0 wt % sample in addition to ~5 nm nanoparticles (Figure 9B). It is a general trend in heterogeneous photocatalysis that highly dispersed catalytic species such as Pt lead to improved performance.<sup>1f,5b,23,25,30,37–42</sup> Another possibility is that recombination between hydrogen atoms (H<sup>•</sup>) on the surface of the Pt catalyst and Ru(bpy)<sub>3</sub><sup>3+</sup>, which has been pointed out by Grätzel et al.,<sup>44</sup> increases at higher loading, contributing to a decrease in H<sub>2</sub> evolution activity.

**Photocatalyst Deactivation.** Figure 10 shows the time course of H<sub>2</sub> evolution from the optimized Pt-loaded NS-K<sub>4</sub>Nb<sub>6</sub>O<sub>17</sub>/Ru(bpy)<sub>3</sub><sup>2+</sup>/EDTA system under intermittent visible light irradiation ( $\lambda > 420$  nm). Even under the optimal conditions, the rate of H<sub>2</sub> production decreased gradually with

(36) (a) Mulvaney, P.; Grieser, F.; Meisel, D. *Lungmuir* **1990**, *6*, 567. (b) Ford, W. E.; Rodgers, M. A. J. *J. Phys. Chem.* **1994**, *98*, 3822.  
 (37) Sakata, T.; Kawai, T.; Hashimoto, K. *Chem. Phys. Lett.* **1982**, *88*, 50.  
 (38) Pichat, P.; Mozzanega, M. N.; Disdier, J.; Herrmann, J. M. *Nouv. J. Chim.* **1982**, *6*, 559.  
 (39) Reber, J. F.; Meier, K. J. *J. Phys. Chem.* **1986**, *90*, 824.  
 (40) Ohtani, B.; Iwai, K.; Nishimoto, S.; Sato, S. *J. Phys. Chem. B* **1997**, *101*, 3349.  
 (41) Hara, M.; Nunoshige, J.; Takata, T.; Kondo, J. N.; Domen, K. *Chem. Commun.* **2003**, 3000.  
 (42) Bao, N.; Shen, L.; Takata, T.; Domen, K. *Chem. Mater.* **2008**, *20*, 110.

(43) When the photolysis reaction was carried out using a band pass filter of  $450 \pm 20$  nm, the rate of H<sub>2</sub> evolution was  $3.55 \mu\text{mol} \cdot \text{h}^{-1} \cdot R$  in eq 2 is thus calculated to be ca.  $2.14 \times 10^{18}$  molecules  $\cdot \text{h}^{-1}$ , with  $I$  measured to be ca.  $4.08 \times 10^{19}$  photons  $\cdot \text{h}^{-1}$ . Equation 2 thus gives a value of 10.5% for AQY.

(44) Moser, J.; Grätzel, M. *J. Am. Chem. Soc.* **1984**, *106*, 6557.

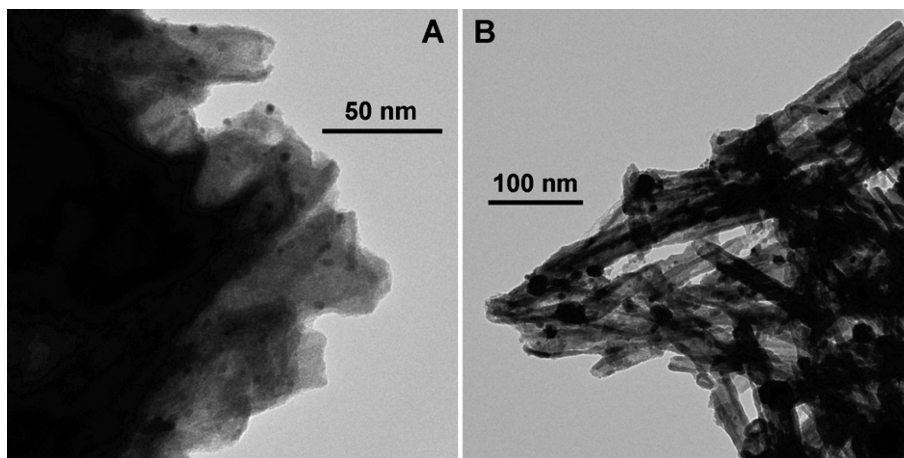


**Figure 9.** TEM images of NS-K<sub>4</sub>Nb<sub>6</sub>O<sub>17</sub> loaded with (A) 0.3 and (B) 5.0 wt % Pt.

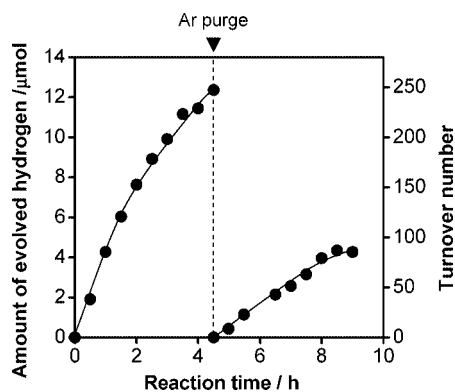


**Figure 10.** Time course of H<sub>2</sub> evolution from 0.3 wt % Pt-loaded NS-K<sub>4</sub>Nb<sub>6</sub>O<sub>17</sub> sensitized by Ru(bpy)<sub>3</sub><sup>2+</sup> with intermittent visible light irradiation ( $\lambda > 420$  nm). Reaction conditions: catalyst, 5.0 mg; aqueous solution (2.0 mL, pH 5.5) containing 10 mM EDTA and 50  $\mu$ M Ru(bpy)<sub>3</sub><sup>2+</sup>; light source, xenon lamp (300 W) with a cutoff filter.

time, although the TON of this reaction exceeded 330. It has been reported that the accumulation of H<sub>2</sub> in the reaction system can have a negative effect on the activity of Pt-loaded photocatalysts. For example, the photocatalytic activities of tantalum oxynitride (TaON)<sup>45</sup> and rhodium-doped strontium titanate (SrTiO<sub>3</sub>:Rh)<sup>46</sup> decrease with accumulation of H<sub>2</sub> in the system. If photogenerated H<sub>2</sub> suppresses the H<sub>2</sub> evolution rate, then the activity should be recoverable by removing the accumulated H<sub>2</sub> from the headspace. In this case, the deactivation can be regarded as reversible. To examine this possibility, the reaction system was purged with Ar after 4.5 h of irradiation and then irradiated again with visible light. The rate of H<sub>2</sub> evolution did not recover, as shown in Figure 10, indicating that irreversible deactivation of the catalytic system occurs in the H<sub>2</sub> evolution reaction. UV–visible spectroscopy revealed that about 73% of the Ru(bpy)<sub>3</sub><sup>2+</sup> molecules in the reaction system were desorbed from the NS-K<sub>4</sub>Nb<sub>6</sub>O<sub>17</sub> surface during 9 h of reaction (see Supporting Information, Figure S3). Over the same time, the pH of the solution increased from 5.5 to approximately

7–8.<sup>47</sup> As electron injection from the excited dye molecules into the semiconductor is indispensable for dye-sensitized H<sub>2</sub> production, the primary cause of the deactivation is the desorption of Ru(bpy)<sub>3</sub><sup>2+</sup> molecules from the surface of NS-K<sub>4</sub>Nb<sub>6</sub>O<sub>17</sub>. The most likely cause of desorption is ion exchange by cationic decomposition products of EDTA. Litter et al. have investigated the photocatalytic decomposition of EDTA using a P25 titania catalyst.<sup>48</sup> In that study, the decomposition products consisted of various organic molecules and ions including glycine, ethylenediamine, ammonium, formaldehyde, and formic, iminodiacetic, oxalic, oxamic, glycolic, and glyoxylic acids, depending on experimental conditions. In the present case, we presume that some of the oxidation products of EDTA (most likely, amine and ammonium species) gradually increase the pH of the solution, and the protonated forms of these molecules displace Ru(bpy)<sub>3</sub><sup>2+</sup> ions from the surface of NS-K<sub>4</sub>Nb<sub>6</sub>O<sub>17</sub>. As a result, the rate of H<sub>2</sub> evolution decreases. Other factors, such as the decomposition of Ru(bpy)<sub>3</sub><sup>2+</sup>, may be secondary causes of deactivation.

The observed deactivation in EDTA solutions is not a serious problem, because the ultimate goal is to combine this H<sub>2</sub> production system with an O<sub>2</sub> production system such as IrO<sub>2</sub>.<sup>1b,10a</sup> Since O<sub>2</sub> evolution on IrO<sub>2</sub> nanoparticle catalysts coupled with Ru(bpy)<sub>3</sub><sup>2+</sup>-based sensitizers proceeds most efficiently at about pH 5,<sup>49</sup> the catalytic system for H<sub>2</sub> evolution should also function efficiently near pH 5. The fact that the sacrificial NS-K<sub>4</sub>Nb<sub>6</sub>O<sub>17</sub>-based system is optimized at pH 5.5 is encouraging in this regard. However, before this system can be coupled to an O<sub>2</sub>-evolving catalyst for overall water splitting, the Pt catalyst must be replaced by one that will not catalyze the H<sub>2</sub>–O<sub>2</sub> recombination reaction.

(45) Hitoki, G.; Takata, T.; Kondo, J. N.; Hara, M.; Kobayashi, H.; Domen, K. *Chem. Commun.* **2002**, 1698.

(46) Konta, R.; Ishii, T.; Kato, H.; Kudo, A. *J. Phys. Chem. B* **2004**, *108*, 8992.

(47) The precise pH of the solution after the reaction could not be measured with a pH meter probe because of the small reaction volume. Therefore, we obtained the approximate pH using pH indicator paper.

(48) Babay, P. A.; Emilio, C. A.; Ferreyra, R. E.; Gautier, E. A.; Gettar, R. T.; Litter, M. I. *Int. J. Photoenergy* **2001**, *3*, 193.

(49) (a) Harriman, A.; Pickering, I. J.; Thomas, J. M.; Christensen, P. A. *J. Chem. Soc., Faraday Trans. 1* **1988**, *84*, 2795. (b) Hara, M.; Waraksa, C. C.; Lean, J. T.; Lewis, B. A.; Mallouk, T. E. *J. Phys. Chem. A* **2000**, *104*, 5275. (c) Morris, N. D.; Suzuki, M.; Mallouk, T. E. *J. Phys. Chem. A* **2004**, *108*, 9115. (d) Hoertz, P. G.; Kim, Y. I.; Youngblood, W. J.; Mallouk, T. E. *J. Phys. Chem. B* **2007**, *111*, 6945.



Although further research including direct measurements of the dynamics of electron transfer needs to be done to achieve a full understanding of this system, the present study clearly demonstrates the effectiveness of nanosheet-based materials for applications in dye-sensitized H<sub>2</sub> production and the importance of surface ion-exchange equilibria in controlling their efficiency. As there are many other oxide semiconductors that can be prepared as nanosheets and scrolls by exfoliation and subsequent restacking, it may be possible to find other materials with improved properties as photocatalysts for H<sub>2</sub> evolution. Research along these lines is currently in progress.

### Conclusions

Oxide semiconductor nanoscrolls, which are prepared by exfoliation of lamellar K<sub>4</sub>Nb<sub>6</sub>O<sub>17</sub> and subsequent restacking, were examined as building blocks of a photocatalytic system for visible light H<sub>2</sub> production. The negatively charged NS-K<sub>4</sub>Nb<sub>6</sub>O<sub>17</sub> binds the cationic Ru(bpy)<sub>3</sub><sup>2+</sup> sensitizer over the pH range of interest for most photocatalytic systems. The higher activity of the NS-K<sub>4</sub>Nb<sub>6</sub>O<sub>17</sub>-based system relative to those based on lamellar K<sub>4</sub>Nb<sub>6</sub>O<sub>17</sub> (H<sup>+</sup>/K<sub>4</sub>Nb<sub>6</sub>O<sub>17</sub>) and P25

titania is due primarily to the high surface area of the nanoscrolls and their ability to bind Ru(bpy)<sub>3</sub><sup>2+</sup>. Transfer of electrons from the sensitizer to the Pt catalyst islands via the single-crystalline nanoscrolls appears to be a facile process. Direct measurements of the electron transfer rates in this system via flash photolysis techniques are expected to contribute to a more quantitative understanding of the kinetics and limitations of photocatalytic systems based on NS-K<sub>4</sub>Nb<sub>6</sub>O<sub>17</sub>.

**Acknowledgment.** This work was supported by the Office of Basic Energy Sciences, Division of Chemical Sciences, Geosciences, and Energy Biosciences, Department of Energy, under contract DE-FG02-07ER15911. K.M. gratefully acknowledges the support of a Japan Society for the Promotion of Science (JSPS) Fellowship.

**Supporting Information Available:** Powder XRD pattern and TEM images of as-prepared NS-K<sub>4</sub>Nb<sub>6</sub>O<sub>17</sub> and UV–visible spectra of the supernatant solution before and after 9 h of reaction. This material is available free of charge via the Internet at <http://pubs.acs.org>.

CM801807B